

DYNAMIC DISPLACEMENT AND STRAIN FIELDS WITHIN TRENCHED SOILS: POST-PROCESSING QUANTITIES FROM INDIRECT-BEM'S FICTITIOUS LOADS

David A. S. Carneiro

david_ascarneiro@hotmail.com

Computational Modeling Methods Laboratory, Federal University of Piauí

Campus Universitário Ministro Petrônio Portella - Ininga, 64049-550, Teresina PI, Brazil

Josue Labaki

labaki@fem.unicamp.br

School of Mechanical Engineering, University of Campinas

200 Mendelejev St, 13083-860, Campinas SP, Brazil

Simone S. Hoefel

simone.santos@ufpi.edu.br

Computational Modeling Methods Laboratory, Federal University of Piauí

Campus Universitário Ministro Petrônio Portella - Ininga, 64049-550, Teresina PI, Brazil

Persio L. A. Barros

persio@fec.unicamp.br

School of Civil Engineering, Architecture, and Urbanism, University of Campinas

224 Saturnino de Brito St, 13083-889, Campinas SP, Brazil

Abstract. This work investigates time-harmonic strain and displacement fields within trenched soils through an Indirect-BEM (IBEM) approach. The method consists of a superposition of Green's functions for surface and buried loads. Solutions for surface loads are used to discretize a rigid plate at the surface of the soil, on top of which time-harmonic vertical loads are applied. Solutions for buried load are used together with zero-stress boundary conditions to model the presence of trenches in the soil. The soil is modeled as homogeneous isotropic or transversely isotropic half-spaces, for which classical Green's functions are available in the literature. Stress and displacement fields within the trenched half-space containing a surface plate are related through sets of fictitious loads. Post-processing from these loads yield quantities such as the displacement field anywhere in the half-space. This work uses these post-processed quantities to study how the ground vibration propagating from the loaded plate is affected by the presence of trenches.

Keywords: Indirect-BEM, Dynamic Soil-Structure Interaction, Trenches and Barriers, Wave Propagation in Soil

1 Introduction

The Indirect-BEM (IBEM) is an alternative formulation for the classical (Direct-) Boundary Element Method, in which displacement and traction fields are connected through fictitious loads, rather than directly through singular auxiliary solutions. The solution for a given boundary value problem arises from the solution of the fictitious loads that satisfy simultaneously the displacement and traction fields at discrete points of the boundary of the problem. Displacement and traction fields, and quantities deriving from them, can be computed anywhere else through post-processing of the fictitious loads. This work illustrates the accuracy of this technique for the case of a homogeneous half-space containing trenches of different lengths. The trench surrounds a rigid circular plate at the surface of the half-space, on which a time-harmonic vertical load is applied. Green's functions necessary for modeling the soil part are obtained from a classical solution in terms of Hankel transforms (Rajapakse and Wang [1]). Continuity and equilibrium conditions throughout the foundation-soil interface are established at discrete points, which results in an elegant algebraic expression involving external loads and fictitious loads at the interfaces. The present model considers contact tractions to be uniformly distributed within each discretized interface segment, which nonetheless yields accurate results.

Barros [2] proposed a boundary element model of a rigid circular plate under an external vertical dynamic excitation surrounded by a buried circular trench with negligible thickness in order to analyze the influence of trench position and depth in its vibration attenuation efficiency. The influence of soil properties was also investigated. An alternative to open trenches was presented in Barros and Mesquita [3] in which the screening capability of a concrete-filled trench was compared with that of an empty trench. This analysis showed that the attenuation performance of an empty trench is significantly higher than that of a filled one.

In many applications of a single trench, the minimum depth to yield any significant attenuation performance can reach tens of meters, which results in an open trench stability problem. As alternative solution, models encompassing multiple trenches were developed. An implementation of Barros model was proposed by Barros and Mesquita [4] which presented a second trench surrounding the surface plate. The efficiency of double trench isolation was compared with that of a single trench. A similar model was presented in Barros and Mesquita [5], who investigated the isolation capability of double circular trenches surrounding the surface plate under an external horizontal dynamic load. In both cases, results showed an increase in the isolation efficiency of double trenches in comparison with that of a single trench. All those works evaluated the efficiency of buried trenches only through analyses of the displacement fields along the ground surface.

In this work, the resulting fictitious loads from the discretized half-space are used to compute displacement fields in a mesh within the half-space. Dynamic displacement and strain fields are obtained from these for an area of the half-space encompassing the foundation and the trench. The results for an untrenched isotropic half-space show clearly undisturbed, outward-propagating pressure and shear waves, the length of which matches the calculated wavelength in that medium, as well as a noticeable compliance with Sommerfeld's radiation condition (Sommerfeld [6]). The presence of the trench affects the propagation of both pressure and shear waves significantly, and the degree by which this occurs depends on the length of the trench.

1.1 Statement of the problem

Consider a three-dimensional, transversely isotropic, homogeneous, viscoelastic half-space, the plane of isotropy of which is parallel to its free surface. The medium is described by five independent elastic constants c_{11} , c_{12} , c_{13} , c_{33} , and c_{44} , mass density ρ , and damping factor β . A massless, rigid, circular plate of radius a rests on the surface of the half-space, the center of which is aligned with the origin of the coordinate system. The plate is subjected to a time-harmonic vertical load $F(t)$. A circular trench of radius R , depth h , and zero thickness, surrounds the plate.

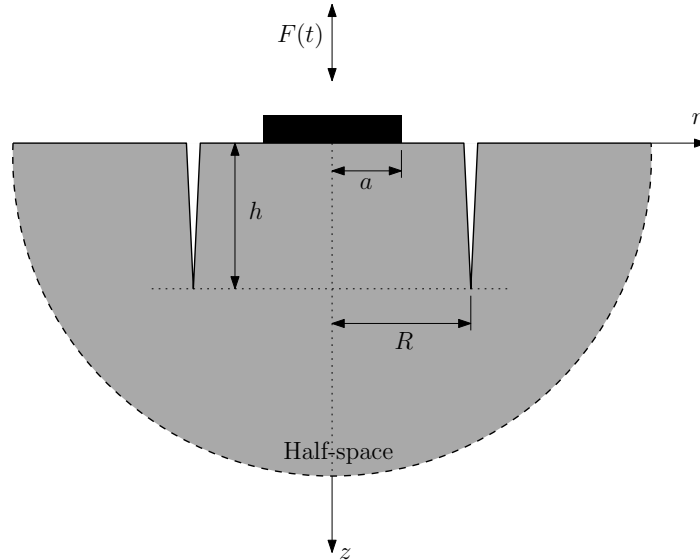


Figure 1. Rigid plate surrounded by circular trench within a homogeneous half-space.

2 IBEM formulation of a trench

A subdomain technique is used with the IBEM formulation of a trench. The half-space divided in two subdomains is shown in Fig. 2. Region 1 encompasses the rigid circular plate and the circular soil delimited by the trench. Region 2 is formed by the remaining soil. This split yields three interfaces: the soil-foundation interface, the trench faces, and regions 1-2.

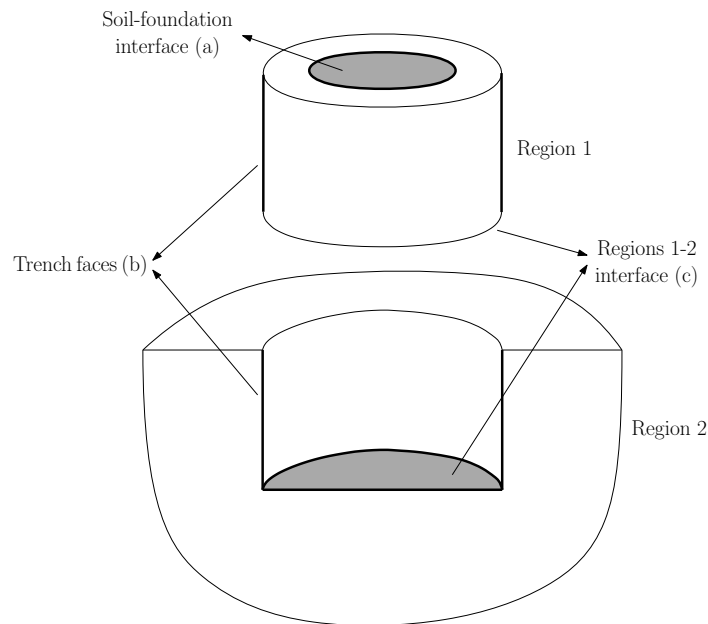


Figure 2. Regions and interfaces of the divided half-space.

Uniformly distributed radial q_r^i and vertical q_z^i fictitious loads are applied at the discretized interface elements of region i . These fictitious loads satisfy simultaneously the displacement and traction fields at the center point of each element. The displacement and traction fields are given respectively by:

$$\mathbf{u}_{ik} = \mathbf{U}_{ik}\mathbf{q}_{ik}, \quad (1)$$

$$\mathbf{t}_{ik} = \mathbf{T}_{ik}\mathbf{q}_{ik}, \quad (2)$$

in which \mathbf{u}_{ik} and \mathbf{t}_{ik} are the vectors of radial u_r , t_r and vertical u_z , t_z displacements and tractions at elements of interface k in region i , \mathbf{q}_{ik} is the vector of radial q_r and vertical q_z fictitious loads, and \mathbf{U}_{ik} and \mathbf{T}_{ik} are, respectively, the matrices of displacement and stress influence functions which are non-singular Green's functions. This formulation uses influence functions for dynamic response of a homogeneous, transversely isotropic half-space due to axisymmetric distributed loads developed by Rajapakse and Wang [1].

The surface plate is subjected to a vertical load. The boundary conditions imposed in the soil-foundation interface (a) are expressed by:

$$(u_{zj})_{1a} = u_0, \quad (3)$$

$$(u_{rj})_{1a} = 0, \quad j = 1, \dots, N_a \quad (4)$$

$$F_z = 4\pi \sum_{j=1}^{N_a} (t_{zj} r_j l_j)_{1a}, \quad (5)$$

in which N_a is the number of elements in the soil-foundation interface, u_0 is the rigid foundation displacement, F_z is the vertical load applied to the plate, r_j is the radial position of the middle of element j , and l_j is the radial width of element j . In the matrix form, this can be written as:

$$\mathbf{u}_{1a} = \mathbf{C}\mathbf{u}_0, \quad (6)$$

$$\mathbf{f} = \mathbf{D}\mathbf{t}_{1a}. \quad (7)$$

In this model, the trenches are formulated as traction-free surfaces embedded in the soil. That is, boundary conditions established at interfaces (b) are:

$$\mathbf{t}_{1b} = 0, \quad (8)$$

$$\mathbf{t}_{2b} = 0. \quad (9)$$

This model assumes that regions 1 and 2 are perfectly bonded at interface (c). Displacement compatibility and traction equilibrium are imposed and result in:

$$\mathbf{u}_{1c} - \mathbf{u}_{2c} = 0, \quad (10)$$

$$\mathbf{t}_{1c} + \mathbf{t}_{2c} = 0. \quad (11)$$

Combining Eqs. 1, 2, 6 and 7, the matrix system for region 1 which involves all three interfaces, can be represented by:

$$\begin{bmatrix} \mathbf{U}_{1a} & -\mathbf{C} \\ \mathbf{T}_{1b} & 0 \\ \mathbf{T}_{1c} & 0 \\ \mathbf{D}\mathbf{T}_{1a} & 0 \end{bmatrix} \begin{bmatrix} \mathbf{q}_{1a} \\ \mathbf{q}_{1b} \\ \mathbf{q}_{1c} \\ \mathbf{u}_0 \end{bmatrix} = \begin{bmatrix} 0 \\ 0 \\ \mathbf{t}_{1c} \\ \mathbf{f} \end{bmatrix}. \quad (12)$$

The solution of this matrix system together with Eq. 1 yields:

$$\mathbf{u}_{1c} = \begin{bmatrix} \mathbf{U}_{1c} & 0 \end{bmatrix} \begin{bmatrix} \mathbf{U}_{1a} & -\mathbf{C} \\ \mathbf{T}_{1b} & 0 \\ \mathbf{T}_{1c} & 0 \\ \mathbf{DT}_{1a} & 0 \end{bmatrix}^{-1} \begin{bmatrix} 0 \\ 0 \\ \mathbf{t}_{1c} \\ \mathbf{f} \end{bmatrix}, \quad (13)$$

which in compact form gives

$$\mathbf{u}_{1c} = \mathbf{M}_1 \mathbf{t}_{1c} + \mathbf{m}_1 \mathbf{f}. \quad (14)$$

A similar procedure can be applied to region 2:

$$\begin{bmatrix} \mathbf{T}_{2b} \\ \mathbf{T}_{2c} \end{bmatrix} \begin{bmatrix} \mathbf{q}_{2b} \\ \mathbf{q}_{2c} \end{bmatrix} = \begin{bmatrix} 0 \\ \mathbf{t}_{2c} \end{bmatrix}, \quad (15)$$

then

$$\mathbf{u}_{2c} = \mathbf{U}_{2c} \begin{bmatrix} \mathbf{T}_{2b} \\ \mathbf{T}_{2c} \end{bmatrix}^{-1} \begin{bmatrix} 0 \\ \mathbf{t}_{2c} \end{bmatrix}, \quad (16)$$

or

$$\mathbf{u}_{2c} = \mathbf{M}_2 \mathbf{t}_{2c}. \quad (17)$$

The boundary conditions at the interface (c) presented in Eqs. 10 and 11, yield $\mathbf{u}_{1c} = \mathbf{u}_{2c}$ and $\mathbf{t}_{1c} = -\mathbf{t}_{2c}$. The final system of equations is given by:

$$(\mathbf{M}_1 + \mathbf{M}_2) \mathbf{t}_{1c} = -\mathbf{m}_1 \mathbf{f}. \quad (18)$$

The solution of this system of equations furnishes the tractions $\mathbf{t}_{1c} = -\mathbf{t}_{2c}$ at interface (c), which can be used to calculate the fictitious loads \mathbf{q}_{ik} and the foundation displacement \mathbf{u}_0 , through equations 12 and 15.

3 Post-processing displacement and strain fields

The IBEM formulation for the surface plate and a buried trench furnishes the fictitious loads applied at each discretized interface element. Consequently, the displacement fields and quantities deriving from this can be evaluated anywhere in the half-space through post-processing from those loads. The displacement fields at each region are obtained by the Eq. 1 in which relates the displacement fields at nodes of a mesh within the half-space and fictitious loads through influence functions. Strain fields throughout the half-space are obtained using interpolation of displacements between nodes of the elements in the mesh. An undeformed and deformed square element of the mesh is shown in Fig. 3.

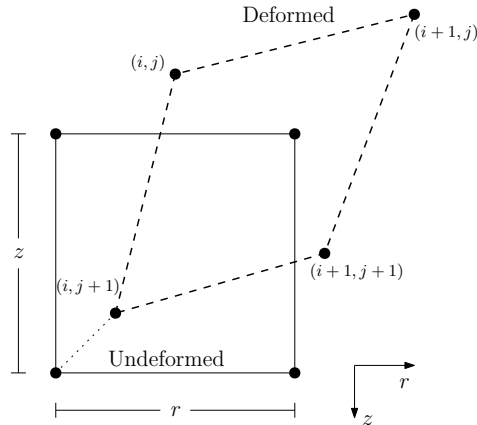


Figure 3. Undeformed and deformed square element.

Each element has volumetric and shear strain that are, for axisymmetric strain, given respectively by:

$$\epsilon = \epsilon_{rr} + \epsilon_{zz}, \quad (19)$$

$$\gamma = \epsilon_{rz}, \quad (20)$$

in which ϵ_{rr} and ϵ_{zz} are respectively the normal strain in direction r and z , and ϵ_{rz} is the distortion of the element. Supposing the deformation is very small, those normal strain and the distortion can be written as:

$$\epsilon_{rr} = \frac{u_r^{(i+1,j)} - u_r^{(i,j)}}{r} + \frac{u_r^{(i+1,j+1)} - u_r^{(i,j+1)}}{r}, \quad (21)$$

$$\epsilon_{zz} = \frac{u_z^{(i,j+1)} - u_z^{(i,j)}}{z} + \frac{u_z^{(i+1,j+1)} - u_z^{(i+1,j)}}{z}, \quad (22)$$

$$\epsilon_{rz} = \frac{1}{2} \left(\frac{u_r^{(i,j+1)} - u_r^{(i,j)}}{z} + \frac{u_z^{(i+1,j+1)} - u_z^{(i,j+1)}}{r} \right), \quad (23)$$

in which $u_r^{(k,m)}$ and $u_z^{(k,m)}$ are respectively the radial and vertical displacements at node (k, m) , and r and z are respectively the horizontal and vertical lengths of the undeformed element. Note that the sum of Eqs. 21 and 22 are taken to represent the volumetric strain and Eq. 23 the shear strain for an element.

4 Numerical results

Figure 4a shows the volumetric strain within an isotropic half-space without a trench. The corresponding case with a trench of radius $R/a=3$ and depth $h/a=1$ is shown in Fig. 4b. Please download the file with animations by clicking [\[here\]](#). All figures in this section are animations, which can be played in the PDF version of this article.

(a) Untrenched soil

(b) Trenched soil

Figure 4. Volumetric strain throughout the half-space with and without a trench of $h/a=1$.

Yellow shades in these figures correspond to positive values of volumetric strain, while blue shades indicate negative volumetric strain. Dark shades of blue indicate the propagation of compressive waves and a parcel of Rayleigh waves around the free surface resulting from the external load. The animation shows that wave propagate from the source (the plate) without reflection, which shows the compliance of the model to Sommerfeld's Radiation condition. Figure 4b shows that the presence of the trench causes compressive waves to propagate mostly in the vertical direction. In this case of short trench, part of the waves propagates around the bottom of the trenches through to the other side. The amplitude of these waves beyond the trench is almost that of untrenched portions of the half-space under the plate. This indicates that this length of trench is insufficient to block ground vibrations for this intensity of excitation.

Figure 5 considers the incorporation of a longer trench ($h/a=4$). These results show a strong reduction of the amplitude of the waves beyond the trench, towards shades of green, which indicate values of strain around zero. This shows an increased ability of this trench to control propagation of waves from the plate.

Figure 5. Volumetric strain within the half-space with a trench of $h/a=4$.

A comparison between Figs. 4a and 5 shows that the presence of the deep trench causes most of the propagating energy to occur in the vertical direction, differently than in the untrenched half-space, in which this propagation occurs in all direction more uniformly.

Conversely, Fig. 6 shows the shear strain within the half-space for the case of a short trench ($R/a=3$, $h/a=1$) and its untrenched half-space counterpart. The mirrored colors in these results correspond to the distortion of the medium to be happening in different directions in each side, which is physically consistent.

(a) Untrenched soil

(b) Trenched soil

Figure 6. Shear strain throughout the half-space with and without a trench of $h/a=1$.

Figure 6a shows that shear strain waves propagate mostly in the horizontal direction. The fading of the colors for points deep within the half-space indicate that shear waves are more prominent towards the free surface. At the surface, these waves correspond to the shear component of the Rayleigh waves. The pressure component had been shown in Fig. 4a.

Figure 6b shows that a trench of depth $h/a=1$ is too short to block shear waves as well. The amplitude of excitation due to these waves beyond the trench is of the order of those within the trenched area.

Finally, Fig. 7 shows the efficiency of a longer trench ($h/a=4$) in blocking shear waves originating from the plate. Strain fields beyond the trench in this case are closer to shades of green (closer to zero) than in the short trench case. One may also point out the inversion of signal of the shear waves as they reach the trench walls, indicating their reflection.

Figure 7. Shear strain within the half-space with a trench of $h/a=4$.

4.1 Effect of anisotropy

This section considers the effect of the anisotropy of the soil in shear and volumetric strains of the soil. This analysis considers $c'_{11} = 6.0$, $c'_{12} = 1.0$, $c'_{13} = 2.648$ and $c'_{33} = 3.0$ ($c'_{ij} = c_{ij}/c_{44}$). Figure 8 shows the volumetric strain field within an untrenched transversely isotropic half-space and within a half-space with a long trench ($h/a=4$). A comparison between these results and their isotropic half-space counterparts (Fig. 5) shows that the propagation of pressure waves is flattened in the vertical direction, which is physically consistent with this medium being stiffer horizontally. Higher elasticity modulus in a given direction correspond to more quickly-propagating waves in that direction. In this case, in which the energy would mostly propagate in the horizontal direction without the presence of a trench, a stark difference is observed in the wave propagation after the inclusion of the trench. This difference is larger than in the isotropic case, in which waves propagate in all directions more uniformly.

(a) Untrenched soil (b) Trenched soil

Figure 8. Volumetric strain within the half-space with a trench of $h/a=4$.

Figure 9 shows the corresponding shear strain fields in the untrenched and trenched transversely isotropic half-space. The effect of anisotropy in the strain fields is less significant in this case than in the case of volumetric strain fields.

(a) Untrenched soil (b) Trenched soil

Figure 9. Shear strain within the half-space with a trench of $h/a=4$.

5 Concluding remarks

This article presented volumetric and shear strain fields within trenched and untrenched soils supporting a surface plate foundation. These quantities were obtained through post-processing from fictitious loads of an indirect formulation of the boundary element method. The results show physical consistency of the model in describing wave propagation phenomena and complying with Sommerfeld's Radiation Condition. The model contributes to our understanding of geotechnical solutions for wave propagation control.

Acknowledgements

The research leading to this work has been funded by the São Paulo Research Foundation (Fapesp) through grant 2017/01450-0. The support of Unicamp and UFPI is also gratefully acknowledged.

References

- [1] Rajapakse, R. N. K. D. & Wang, Y., 1993. Green's functions for transversely isotropic elastic half space. *Journal of Engineering Mechanics*, vol. 119, n. 9, pp. 1724–1746.
- [2] Barros, P. L. A., 2005. Dynamics of a rigid disk foundation surrounded by a trench in a transversely isotropic soil. In *XXVI Iberian Latin American Congress on Computational Methods in Engineering*, Guarapari, Espírito Santo, Brasil.
- [3] Barros, P. L. A. & Mesquita, E., 2008. Screening of surface waves from foundations subjected to dynamic loads by rigid barriers. In *Proceedings of the International Conference of the Engineering Mechanics Institute*, ASCE, Minneapolis, MN, USA.
- [4] Barros, P. L. A. & Mesquita, E., 2007. Screening efficiency of double circular trenches as active isolation for surface foundations subjected to dynamic loads. In *Proceedings of the 18th Engineering Mechanics Division Conference*, ASCE, Blacksburg, VA, USA.
- [5] Barros, P. L. A. & Mesquita, E., 2009. The response of an elastic half-space with circular trenches around a rigid surface foundation subjected to dynamic horizontal loads. In *Proceedings of the 10th International Conference on Boundary Element Techniques (BETEQ)*, Athens, Greece.
- [6] Sommerfeld, A., 1949. *Partial differential equations in physics*. Academic Press.